ECH Power Deposition at 3rd Harmonic in high Elongation TCV Discharges Sustained by 2nd Harmonic Current Profile Broadening

A. Pochelon[1], G. Arnoux[1], Y. Camenen[1], A. Scarabosio[1], S. Alberti[1], F. Hofmann[1], A. Manini[1], R. Behn[1], P. Bosshard[1], P. Blanchard[1], S. Coda[1], T.P. Goodman[1], M.A. Henderson[1], J.-Ph. Hogge[1], A. Karpushov[1], J.-M. Moret[1], E. Nelson-Melby[1], L. Porte[1], O. Sauter[1], A. Sushkov[2], M.Q. Tran[1].

1) Centre de Recherches en Physique des Plasmas, Association EURATOM-Confédération Suisse, Ecole Polytechnique Fédérale de Lausanne EPFL, 1015 Lausanne, Switzerland
2) RRC Kurchatov, Moscow

e-mail contact of main author: Antoine.Pochelon@epfl.ch

Abstract. This paper summarises the present effort aimed at developing high elongation heated discharges and testing their confinement properties at normalised currents for which the highest ideal MHD βlimits are predicted. 2nd harmonic (X2) far off-axis ECH/CD is used to stabilise the plasma vertically at high elongation by broadening the current profile in stationary conditions (during the current flat top and over several current diffusion times). Current broadening is maximal for a power deposition in a narrow region (~a/5), for a finite toroidal injection angle and for high plasma density using upper lateral launchers to minimise refraction. In these discharges which are twice X2 overdense in the centre, 3rd harmonic (X3) is injected from a top launcher to deposit power in the centre and increase the central pressure, simultaneously with far off-axis X2. Using modulated X3, full absorption is measured by the diamagnetic probe. Absorption higher than calculated by thermal ray tracing is occasionally found, indicating absorption on the electron bulk as well as in the suprathermal electron population sometimes with a hollow deposition profile. The high sensitivity of the power coupling to the beam angle stresses the need for developing a mirror feedback scheme [1] to increase the coupling efficiency in transient heating scenarios.

1. Introduction

Plasma shaping, and in particular elongation, is a means to improve tokamak performance [2]. Highly elongated discharges tend to be vertically unstable and can only be stabilised by providing sufficient current density close to the plasma edge [3]. For Ohmic discharges, this is achieved by operating at a low safety factor q_{edge} ($2.2 < \kappa < 2.8$, $I_N = I_p/aB \sim 2.8$-3.5MA/mT). However, in order to reach maximum β-values predicted by ideal MHD for highly elongated plasmas, one has to produce discharges at intermediate I_N values, of the order of 2MA/mT. For these values Ohmic discharges are vertically unstable, but TCV plasmas can be maintained stable by current profile broadening using far off-axis 2nd harmonic X-mode ECH/CD (X2) [4-7]. This leads to highly elongated discharges ($\kappa \sim 2.48$) at low current and high safety factor ($I_N \sim 1.05$MA/mT, $q_{edge} \sim 10$) using 3/4 of the upper lateral port installed EC power [8]. X3 power has been coupled to the plasma in ohmic condition and in combination with X2 ECW [9-12]. In this paper we are using simultaneously far off-axis 2nd harmonic ECW for plasma shaping and 3rd harmonic (X3), with the aim of measuring and optimising the coupling of X3 power deposition.

2. Experimental set-up

TCV is equipped with 4.5MW ECH nominal power for 2s pulse length: 3MW at the 2nd harmonic and 1.5MW at the 3rd harmonic. The X2 system consists of six 475kW gyrotrons at 82.7GHz with six independent low field side (LFS) launchers, four upper lateral and two equatorial, steerable during the discharge. The X3 system consists of three 420kW gyrotrons at 118GHz using a single top launcher, also steerable during the discharge. The cut-off densities of X2 and X3 waves are 4.25 and 11.5 10^{19}m^{-3} respectively.

Using power modulation techniques, the total absorbed power is measured by a diamagnetic loop (DML) [13,14], and the local deposition is measured with a 64 channels soft X-ray wire chamber (MPX) filled with Xenon, sensitive between 2-25keV (10% efficiency limits) [14,15]. The level of the suprathermal electron population is obtained by comparing HFS ECE radiation temperatures, $T_{e\,ECE}$, with the Thomson temperatures T_e [10].

3. High elongation stabilised by far off-axis ECH/CD X2

Typical time traces of a highly elongated plasma produced with off-axis ECH are shown in Fig. 1. X2 power is launched on a plasma with intermediate elongation, keeping the pre-programmed quadrupole and hexapole fields constant. The X2 power is deposited far off-axis ($\rho_{dep}=(V_{dep}/V_{max})^{1/2}>0.5$), using upper lateral launchers with a short beam path in the plasma to minimise refraction effects while the plasma reaches high elongation, Fig. 2. The local EC power deposition leads to a local increase in temperature and conductivity, hence to a broadening of the inductive current profile (ECCD and bootstrap currents are negligible, ~8% in this case). As a result, the plasma elongation κ increases on a typical current diffusion time (~0.2s). The main current profile indicator, the internal inductance l_i, decreases when the current profile is broadened or when the elongation is increased. The main contribution to the change in l_i is due to the current profile change (~3/4) [16]. The location of ECH deposition and the plasma first-pass power absorption are computed with the ray tracing code TORAY-GA [17]. The experimental results are compared to those of the fixed boundary transport code PRETOR [18] based on the Rebut-Lallia-Watkins model [18,19]. Both experiment and PRETOR simulation show that the optimal location of the EC power deposition for broadening the current profile is restricted to the region $0.55<\rho_{dep}<0.7$, Fig. 3 [16]. For $\rho_{dep}<0.55$, the current profile broadening effect is reduced, and for $\rho_{dep}<0.4$ the ECH power produces current profile peaking. For $\rho_{dep}>0.75$, the ECH power is both incompletely absorbed in the first-pass and inefficiently confined, reducing its effect on the current profile substantially. The values of the internal inductance computed by LIUQE and the ones computed by PRETOR differ slightly, due to the choice of the current profile functional in the LIUQE reconstructions, optimised for ohmic profiles. Operation at higher current I_N~2, and consequently higher ohmic power, requires proportionally more X2 power to broaden the current profile, hence the need for maximising the efficiency. The dependence of current profile broadening by off-axis X2 ECH on other parameters have been investigated [16].
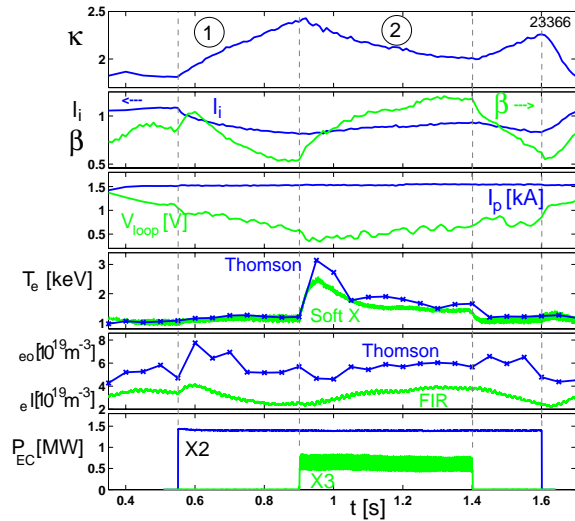

FIG. 1
Phase (1): preparation of a high n_e high κ target with far off-axis ECCD (X2) applied during the current plateau.
Phase (2): addition of X3 (0.63MW average, 50% modulation) to increase the central pressure.
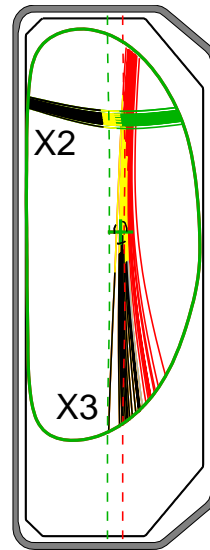
FIG. 2
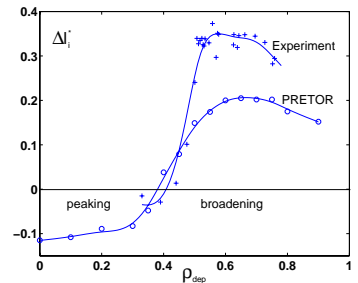*Far off-axis X2 and X3 beams in elongated plasma (#23366, t=0.95s)*

FIG. 3
Current profile change versus radial deposition location ρ_{dep} (I_p=300kA, P_{abs}=1MW, n_{eo}~2.5 $10^{19}m^{-3}$).

Operation at high plasma density, even overdense to X2 in the core, is observed to improve the efficiency of off-axis deposition for increasing plasma elongation, Fig. 4a: for constant injected power, higher elongation is obtained at higher density. This enhancement results firstly from the improvement of confinement with density, which can be seen in the
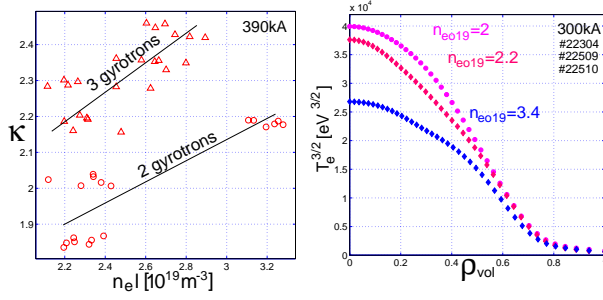
FIG. 4a & 4b   High density operation:
a) *increase of κ with density at constant EC power,*
b) *the temperature deduced resistivity profile, an indication of the current profile, is flattened and therefore broadened with density.*
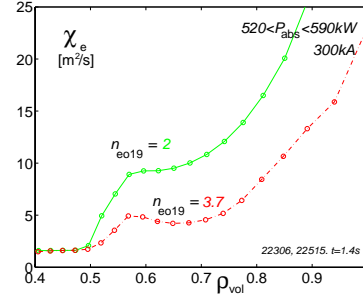

FIG. 5   Current diffusivity χ_e for low ($n_{eo}\sim 2\ 10^{19}m^{-3}$) and high density ($n_{eo}\sim 3.6\ 10^{19}m^{-3}$) and at similar absorbed power, respectively $P_{abs}\sim 520$ and $590 kW$ ($\rho_{dep}\sim 0.54$).

mal diffusivity profiles obtained from power balance, Fig. 5. At the higher densities, the χ_e profile is comparably reduced outside the deposition location, as expected from the usual improvement of confinement with density. This corresponds to an electron confinement time τ_{Ee} increase from 5 to 6ms. The enhancement results, secondly, from an increase by more than an order of magnitude of the electron to ion power transfer P_{ei} with density, peaked on axis, which tends to flatten the current profile. In the absence of a direct measurement of the current profile, two pieces of evidence seem to confirm this hypothesis. First, the temperature profile (hence the resistivity profile, proportional to $T_e^{3/2}(\rho)$) is flattened, Fig. 4b. The second piece of evidence comes from MHD activity. At low density, with off-axis heating at low current, 300kA, sawteeth are lost during the elongation ramp-up when $q_o>1$, without noticeable mode activity. At high density, internal mode activity occurs at the $q_o\sim 1$ crossing, and can persist during the full discharge. Such mode activity is analysed using the MPX [15]. An m=1, 2, 3 mode structure inside the inversion radius, Fig. 6, is found, with a slowly decreasing m-spectrum, where the m=2 and 3 mode amplitude are respectively 70% and 20% of the m=1 amplitude, a typical signature of a flat current profile [20].

A further enhancement of X2 efficiency can be obtained by using ECCD ($\varphi\sim\pm 10^o$), thus increasing the suprathermal level.

Optimal conditions for current profile broadening require deposition in a narrow layer $0.55<\rho_{dep}<0.7$, high density operation and some toroidal component of the injection angle. The use of far off-axis X2 ECH in high-density discharges, up to $8\ 10^{19}m^{-3}$ on axis, twice cut-off density, has allowed us to extend the range of elongated equilibria substantially at intermediate currents, Fig. 7.
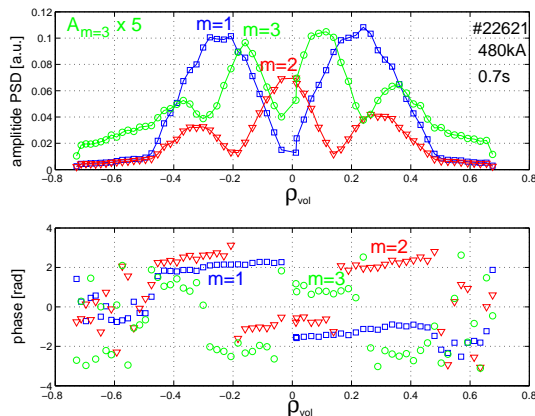

FIG. 6 Mode activity m=1,2,3 inside inversion radius $\rho_{inv}=0.4$, from the 64 channel soft X-ray multiwire proportional chamber diagnostic.

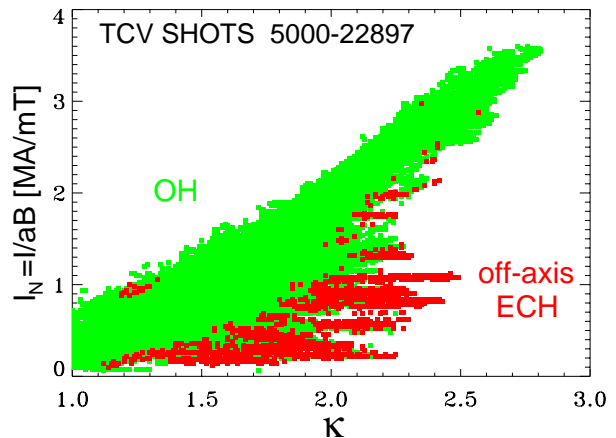*FIG. 7 Range of TCV operation: Ohmic discharges (green) and ECH (red). Off-axis ECH allowed reaching κ=2.48 at low I_N.*

4. X3 power deposition in high elongation discharges

High-elongation high-density discharges, overdense to X2 in the core, are developed ultimately for β-limit and confinement studies. They provide the target plasmas for X3 heating and deposition studies. The discharges have high $n_e T_e$ to maximise X3 absorption and high κ to enhance the absorption by the geometrical effect of shallow incidence on the resonance.

In discharge 23366, see Fig. 1 (390kA, φ_{X2}=+10°, n_{eo}~6->7 $10^{19}m^{-3}$, P_{abs_X2}= 1.41MW deposited at ρ_{dep}= 0.7 to 0.5), we apply 0.63MW average X3 power with half of the power modulated at 337Hz. The elongation reached with X2, κ_{max}~2.43, is limited by vertical stability. Later, during the X3 phase, the central deposition peaks the current profile. The resulting increase of l_i and decrease of κ can only be partly compensated by the shaping coils: keeping the elongation constant, while X3 peaks the current profile, leads to an increase of the vertical instability growth rate, limiting the maximal stable elongation.

The optimal poloidal mirror angle θ_{X3} is found by maximising the soft X-ray temperature in a mirror angle sweep. The optimal X3 power modulation frequency (337Hz), yielding reliable results for both the DML and MPX, gives a phase of the response close to 90°.
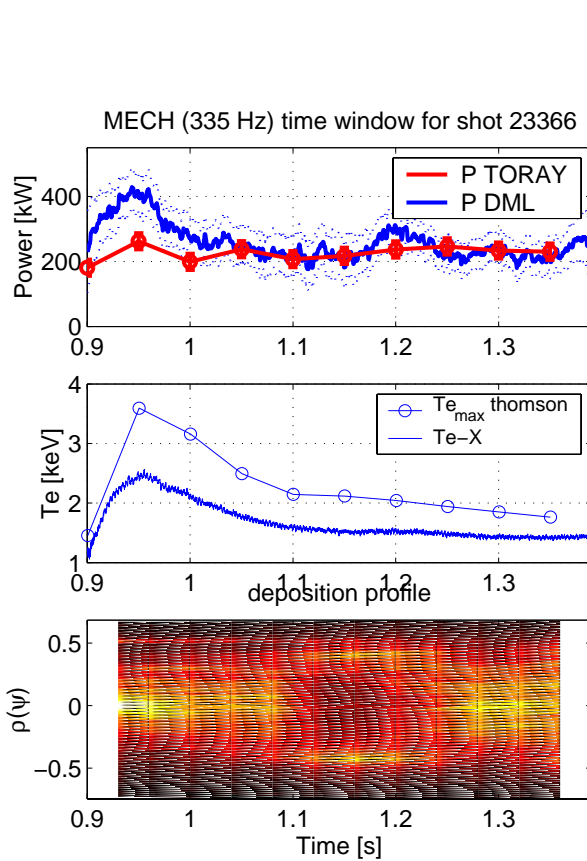

FIG. 9 X2 and X3 beams
a) at start of X3 (n_{eo}= 5.8 $10^{19}m^{-3}$) and
b) at t=1.25s (n_{eo}=6.4 $10^{19}m^{-3}$)

FIG. 8
a) X3 absorbed power from DML and from ray tracing.
b) Electron temperature from Thomson and soft X-ray,
c) Power deposition profile on the MPX, showing different power deposition profile width, from peaked to hollow.
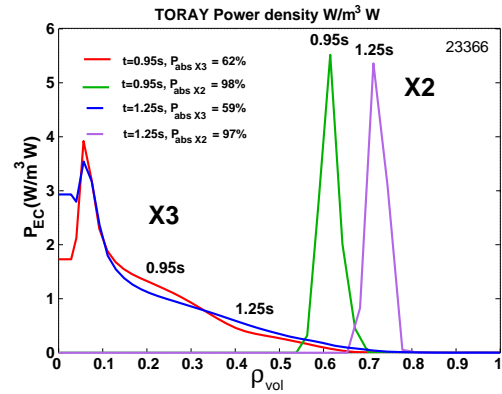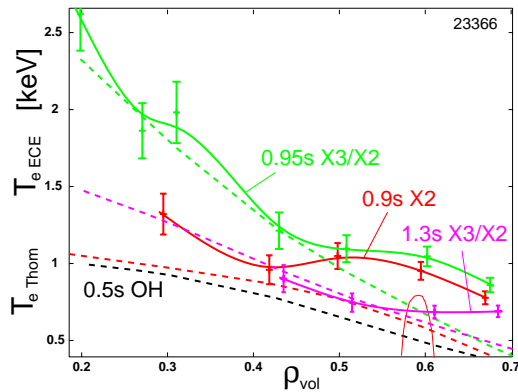

FIG. 10 $T_{e\,ECE}$ (plain) > $T_{e\,Thomson}$ (dashed) profiles indicating suprathermal emission during X2/X3:
1) t=0.5s, ohmic $T_{e\,Thom}$,
2) t=0.9s, X2: $T_{e\,ECE}$ max. just inside ρ_{dep}=0.59, schem. indicated, peaking toward axis, remark $T_{e\,Thom}(\rho)$ broadened by X2,
3) t=0.95s, X3/X2: $T_{e\,ECE}$ ~ $T_{e\,Thom}$ in centre, bigger at ρ_{dep}>0.5; strong X3 bulk heating
    t=1.3s, X3/X2: $T_{e\,ECE}$ > $T_{e\,Thom}$ at ρ_{dep}>0.6, centre unknown.

The power deduced from the DML is identical to that from ray tracing for most of the time slices, which implies a fully thermal plasma, Fig 8. For these times the deposition profile, which is similar to the one deduced from ray tracing, is monotonic and peaked on axis, Fig 9. There are exceptions: at the beginning of X3, a remarkably high T_e is reached together with a very peaked MPX deposition profile. Later, at t=1.25s, a second, smaller T_{eX} maximum is observed, this time associated with a very hollow deposition profile, not accounted for by thermal ray tracing calculations. The hollow deposition and $P_{DML}>P_{Toray}$ indicates again suprathermal absorption. The presence of suprathermals is confirmed by $T_{ECE}/T_{Thomson}>1$, already during X2, and extends over most of the X3 heating period. The T_{ECE} profile evolution in Fig. 10 shows that the maximum of suprathermals during X2 peaks just inside the X2 deposition location and toward the centre of the discharge. At the beginning of X3, the profile rises everywhere, correlated with full absorption as measured by the DML. Later, an annular suprathermal emission forms at $\rho_\psi=0.65$, simultaneous with the annular deposition measured at $\rho_\psi{\sim}0.4$ on the MPX.

These experiments show that the absorption is very sensitive to the mirror angle θ_{X3}. Differences of mirror angle of 0.2^o and variations of the plasma parameters modify the absorbed power significantly, which justifies the development of a feedback system to maintain full power absorption throughout the discharge [1]. However, under these conditions and at half of the nominal power, 630kW, a substantial increase of T_e is measured in the discharge of Fig. 1, with β and $T_i(t)$ profiting from the high density operation.

4. Conclusions

With the help of far off-axis X2 power deposition to broaden the current profile and to elongate the plasma, discharges of high elongation, $\kappa{\sim}2.5$, at $I_N{,}{\sim}1.05$, centrally overdense to X2, have been created and sustained. Higher values of κ and I_N will be achievable with the full X2 power (4 beams) from the upper lateral ports. In these plasmas, X3 power absorption close to 100% has been reached, with typically 60-70% deposited centrally on the bulk, and 20-30% on suprathermal electrons with a broader or hollow radial distribution in presence of suprathermal electrons.

References

[1]   Porte, L., et al., 19th IAEA FEC Conf. IAEA 2002, Lyon, EXP/P5-15.

[2]   Hofmann, F., et al., Phys. Rev. Lett. **81**, (1998) 2918.

[3]   Ericsson, G, Bondeson, A, Ward, D.J., Hofmann, F., Villard, L., Proc. 19th EPS 1992, Vol 16C, Part I, 343.

[4]   Pochelon, A. et al., Proc. 18th IAEA FEC, Sorrento, Italy, IAEA-CN-77 (EXP3/10), (2000) 155.

[5]   Pochelon, A., et al., Nucl. Fusion **41** (2001) 1663.

[6]   Hofmann, F., et al., Plasma Physics and Controlled Fusion, **43** (2001) A161.

[7]   Hofmann, F., et al., Nucl. Fusion **42**, 743-749 (2002).

[8]   Pochelon, A., et al., Proc. 29th EPS Conf, Montreux, June 2002, ECA Vol. 26B (2002) P2.075.

[9]   Alberti, S., et al., Nuclear Fusion **42**, 42 - 45 (2002).

[10] Blanchard, P., Plasma Phys. and Contr. Fusion, **44** (2002) 2231.

[11] Alberti, S., et al., Proc. 29th EPS Conf, Montreux, June 2002, ECA Vol. 26B (2002) P2.073.

[12] Arnoux, G., et al. Proc. 29th EPS Conf, Montreux, June 2002, ECA Vol. 26B (2002) P2.076.

[13] Manini, A., Moret, J.-M., Alberti, S., et al. Plasma Physics and Controlled Fusion, **44** (2002) 139.

[14] Manini, A., Moret, J.-M., Ryter, F. et al., subm. for publ. to Nucl. Fus.; Manini, A., Thesis, LRP 724 (02).

[15] Sushkov, A. et al., Proc. 29th EPS Conf, Montreux, June 2002, ECA Vol. 26B (2002) P4.118.

[16] Camenen, Y., et al., Proc. of EC-12, Aix-en-Provence, France, May 2002, 407.

[17] Matsuda, K., IEEE Trans. Plasma Science. **17** (1989) 6.

[18] Angioni, C., et al., Theory of Fus. Plasmas, Varenna 2000, ISSP-19 (Ed. Comp, Bologna, 2001) 73.

[19] Boucher, D., et al., IAEA TCM Adv. in Simul. & Model. Thermonucl. Plasmas, Montreal (1993) 142.

[20] Duperrex, P-A., et al., Nucl. Fusion **32** (1992) 1161.